Communication

A Self-Assembled Nanofiber Catalyst for Ester Hydrolysis

Mustafa O. Guler, and Samuel I. Stupp

J. Am. Chem. Soc., **2007**, 129 (40), 12082-12083• DOI: 10.1021/ja075044n • Publication Date (Web): 14 September 2007

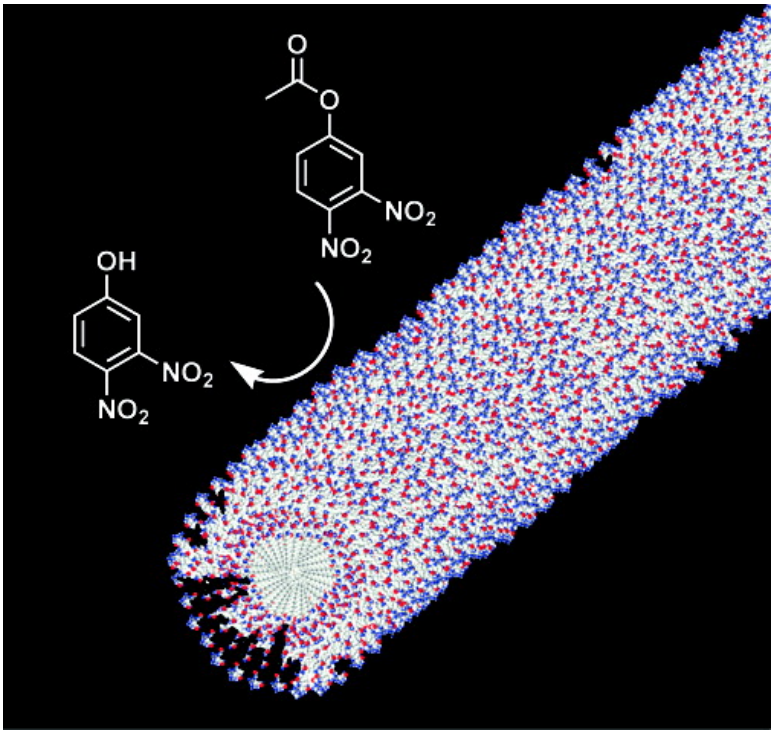

J|A|C|S
COMMUNICATIONS

Published on Web 09/14/2007

A Self-Assembled Nanofiber Catalyst for Ester Hydrolysis

Mustafa O. Guler[†] and Samuel I. Stupp*[,†,‡,§]

Department of Chemistry and Institute for BioNanotechnology in Medicine, Department of Materials Science and Engineering, and Feinberg School of Medicine, Northwestern University, 2220 Campus Drive, Evanston, Illinois 60208

Received July 8, 2007; E-mail: s-stupp@northwestern.edu

The efficiency and selectivity of enzymes have always been a source of inspiration to chemists working on the development of robust synthetic catalysts. Mimicking enzymes with synthetic materials has received considerable attention from both chemists and biologists.[1] Particles that could emulate enzymes have been used to present reactive sites, for example, supramolecular systems derived from polymers,[2] nanostructures,[3,4] and artificial proteins.[5] Most of the synthetic particles investigated have spherical symmetry and lack the internal order which is characteristic of proteins. The use of imidazolyl groups in artificial catalysts has been popular given the presence of histidine residues at the catalytic site of several hydrolytic enzymes including acetylcholine esterase,[6] chymotrypsin,[7] trypsin,[8] and kidney dialkylfluorophosphatase.[9] A considerable increase of reaction rates has been observed upon aggregation of active sites, presumably due to the increase in concentration of reaction loci and cooperativity among functional groups.[10]

In the present study, we demonstrate hydrolysis of a model ester on the surface of nanofibers formed by aggregation of peptide amphiphiles. Peptide amphiphiles (PAs) have been previously shown to self-assemble into nanofibers by hydrophobic collapse of their alkyl tails and β-sheet formation among their peptidic segments.[11−14] We explored the ability of these cylindrical supramolecular nanostructures for hydrolysis of 2,4-dinitrophenyl acetate (DNPA). DNPA, a common model compound to study catalytic activity of enzymes and synthetic systems,[15] was selected here as the substrate for esterase activity. Histidine residues were incorporated into the peptide segment of PA molecules to mimic hydrolytic enzymes discussed above. The compounds **1**−**4** (see Chart 1) were prepared using solid-phase peptide synthesis (SPPS) and purified by reverse phase HPLC. Compound **3** contains the same peptide sequence KLLLAAA present in the PA structure with histidine residues attached to the lysine residue as a peptide control molecule without the palmitoyl group to eliminate the strong amphiphilic character of the system responsible for the formation of well-defined cylindrical aggregates. The proline residues were incorporated into the peptide sequences of **2** and **4** in order to prevent β-sheet formation and promote the formation of spherical aggregates of PA molecules.[17] Previous work has also demonstrated that PA molecules containing proline residues readily assemble into spherical aggregates.[16] Compounds **2** and **4** were synthesized as controls of nanostructure shape since cylindrical nanofibers are characteristic structures in aggregated PA molecules that form β-sheets.[18]

Compound **1** was found to be soluble in water at pH 4 and formed self-supporting gels at concentrations greater than 0.1 wt % and pH above 6.5. Gel formation is a strong indication of self-assembly of PA molecules into high-aspect-ratio nanofibers, and

Chart 1. Chemical Structures of the Molecules Used to Create Nanostructures

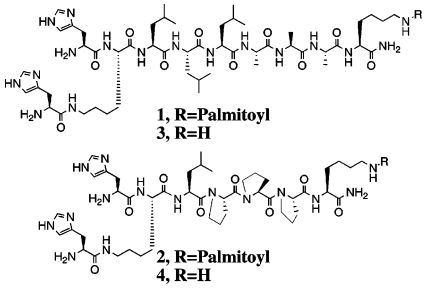

their growth is electrostatically inhibited in acidic pH given the positive charge on the molecules. The electrostatic barrier disappears, and fibers grow spontaneously upon an increase of pH. Transmission electron microscopy (TEM) micrographs of self-assembled compound **1** at pH 7.4 revealed the formation of high-aspect-ratio nanostructures with diameters of 7 ± 1 nm and lengths ranging from hundreds of nanometers to several micrometers (see Figure 1). At the same time, circular dichroism of PA **1** at pH 7.4 revealed a broad peak (n−π* transition) between 205 and 225 nm, which is a signature for the predominant presence of β-sheets (see Figure S1). On the other hand, compounds **2**−**4** were soluble at pH 7.4 and did not form nanofibers but polydisperse spherical aggregates instead with diameters ca. 15−20 nm observed by TEM (see Figure 1). Also as expected, the CD spectra for compounds **2**−**4** revealed a peak (n−π* transition) between 200 and 205 nm which can be attributed mainly to the presence of random coil conformations in the peptide segment of these molecules (see Figure S1).

Hydrolysis of DNPA by imidazolyl-functionalized molecules was monitored by UV−vis spectroscopy at 400 nm to follow the formation of 2,4-dinitrophenol at 25 °C and pH 7.4 in HEPES buffer. The hydrolysis of phenyl acetates was previously reported to be first-order in imidazole concentration.[19] The imidazole directly reacts with the phenyl acetate to form phenol and acylium ion−imidazole complexes. The complex then reacts with water to form acetic acid and imidazole. An imidazole moiety found in the catalytic site of α-chymotrypsin is also known to activate ester hydrolysis, and the Michaelis−Menten enzyme kinetics model was used to calculate the reaction rate constant of the system.[7,20] At high substrate concentration, the catalyst−substrate complex is present in excess in the media, so that the catalyst turnover becomes the rate-limiting step in the enzymatic catalysis reactions. The overall reaction rate is nearly insensitive to further increments in substrate concentration.

The DNPA hydrolysis rates were calculated using varying substrate conditions in the presence of a constant catalyst concentration. The Michaelis−Menten model was used to calculate the hydrolysis rate constant for compound **1** because we observed

[†] Department of Chemistry and Institute for BioNanotechnology in Medicine.
[‡] Department of Materials Science and Engineering.
[§] Feinberg School of Medicine.

10.1021/ja075044n CCC: $37.00

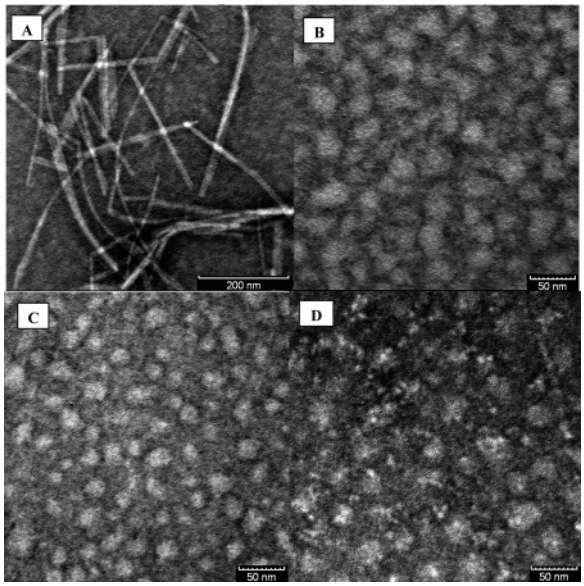

Figure 1. Negatively stained TEM micrographs of **1** (A), **2** (B), **3** (C), and **4** (D) at pH 7.4.

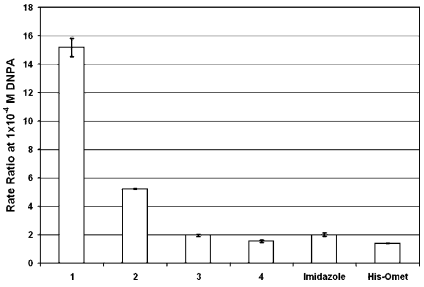

Figure 2. Observed rate increase in DNPA hydrolysis as the level of molecular organization in the catalytic particles is varied.

saturation of the reaction rate at the highest possible concentration of DNPA in the buffer solution used (see Figure S2). The rate constant for DNPA hydrolysis with **1** under self-assembling conditions was found to be $(1.67 \pm 0.13) \times 10^{-2}$ s^{-1} (see Table S1). However, the reaction rate increase was linear as the substrate concentration increases in the presence of molecules **2**−**4**, which form spherical aggregates (see Figure S3). Similar behavior for the hydrolysis of DNPA is observed in the presence of histidine and imidazole, and second-order rate constants were calculated (see Table S2). When the rate of hydrolysis in the presence of 1×10^{-4} M DNPA at pH 7.4 was studied, the rate of hydrolysis with compound **1** was considerably higher than the others (see Figure 2). We believe that the hydrolysis rate enhancement by nanofibers is due to high density presentation of reactive sites with internal order in these supramolecular constructs. We recently reported a high degree of internal order in cylindrical PA nanofibers formed by collapsed β-sheets.[18] Direct evidence of higher density of catalytic sites on nanofibers relative to spherical micelles cannot be directly obtained at this time. However, we expect more highly ordered reactive sites in nanofibers with their strong β-sheet character, and consequently higher density as well. The catalyst−substrate binding on the cylindrical nanofibers can be favored relative to spherical aggregates which are expected to have much less internal order. A higher degree of order in the catalytic particle should reduce the entropic penalty of binding events. Due to a high density of reactive sites in spherical aggregates and possibly even some short range order, hydrolysis of DNPA with **2** is slightly faster than in the presence of **3**, **4**, His-Omet, and imidazole, which suggests that increasing levels of internal organization in the catalyst contribute to efficiency (see Table S2). In **3** and **4**, the potent entropy reducing effect of hydrophobic collapse by palmitoyl segments is absent, and His-Omet and imidazole are of course expected to function as non-supramolecular catalysts.

We conclude that the hydrolysis efficiency of DNPA, a model ester compound, benefits by a high density of reactive sites displayed on the surface of a supramolecular catalytic particle with significant internal order. Considerably higher hydrolysis rate was observed in the presence of internally ordered supramolecular nanofibers as the catalytic particles, compared to catalysts in solution and in spherical aggregates which should have less order. The observations offer a new axis for the design of supramolecular catalysts, suggesting that nanofibers of high aspect ratio and internal order are potentially interesting catalytic devices. The function of these nanostructures can be further increased taking advantage of the possibility of co-assembling molecules in a nanofiber so that various molecular recognition and chemical events can be integrated into a single catalytic system.

Acknowledgment. This work was supported by the U.S. Department of Energy (Award No. DE-FG02-00ER54810) and the National Institutes of Health (Award No. R01 EB003806-01). We thank Steve Soukasene for TEM imaging, James Hulvat and Hakan Usta for helpful discussions.

Supporting Information Available: Experimental details, mass spectra, and hydrolysis rates. This material is available free of charge via the Internet at http://pubs.acs.org.

References

(1) Baltzer, L.; Nilsson, J. *Curr. Opin. Biotechnol.* **2001**, *12*, 355.
(2) Okhapkin, I. M.; Bronstein, L. M.; Makhaeva, E. E.; Matveeva, V. G.; Sulman, E. M.; Sulman, M. G.; Khokhlov, A. R. *Macromolecules* **2004**, *37*, 7879.
(3) Vriezema, D. M.; Aragones, M. C.; Elemans, J.; Cornelissen, J.; Rowan, A. E.; Nolte, R. J. M. *Chem. Rev.* **2005**, *105*, 1445.
(4) Pasquato, L.; Pengo, P.; Scrimin, P. *J. Mater. Chem.* **2004**, *14*, 3481.
(5) Baltzer, L.; Broo, K. S.; Nilsson, H.; Nilsson, J. *Bioorg. Med. Chem.* **1999**, *7*, 83.
(6) Massiah, M. A.; Viragh, C.; Reddy, P. M.; Kovach, I. M.; Johnson, J.; Rosenberry, T. L.; Mildvan, A. S. *Biochemistry* **2001**, *40*, 5682.
(7) Gutfreund, H.; Sturtevant, J. M. *Biochem. J.* **1956**, *63*, 656.
(8) Godzhaev, N. M. *Mol. Biol.* **1984**, *18*, 1163.
(9) Mounter, L. A. *J. Biol. Chem.* **1956**, *219*, 677.
(10) Pengo, P.; Polizzi, S.; Pasquato, L.; Scrimin, P. *J. Am. Chem. Soc.* **2005**, *127*, 1616.
(11) Silva, G. A.; Czeisler, C.; Niece, K. L.; Beniash, E.; Harrington, D. A.; Kessler, J. A.; Stupp, S. I. *Science* **2004**, *303*, 1352.
(12) Hartgerink, J. D.; Beniash, E.; Stupp, S. I. *Science* **2001**, *294*, 1684.
(13) Guler, M. O.; Hsu, L.; Soukasene, S.; Harrington, D. A.; Hulvat, J. F.; Stupp, S. I. *Biomacromolecules* **2006**, *7*, 1855.
(14) Guler, M. O.; Soukasene, S.; Hulvat, J. F.; Stupp, S. I. *Nano Lett.* **2005**, *5*, 249.
(15) Pasquato, L.; Rancan, F.; Scrimin, P.; Mancin, F.; Frigeri, C. *Chem. Commun.* **2000**, 2253.
(16) Guler, M. O.; Claussen, R. C.; Stupp, S. I. *J. Mater. Chem.* **2005**, *15*, 4507.
(17) Li, S. C.; Goto, N. K.; Williams, K. A.; Deber, C. M. *Proc. Natl. Acad. Sci. U.S.A.* **1996**, *93*, 6676.
(18) Jiang, H. Z.; Guler, M. O.; Stupp, S. I. *Soft Matter* **2007**, *3*, 454.
(19) Bruice, T. C.; Sturtevant, J. M. *J. Am. Chem. Soc.* **1959**, *81*, 2860.
(20) Faller, L.; Sturteva, J. *J. Biol. Chem.* **1966**, *241*, 4825.

JA075044N